

Ionospheric Echo Detection in Digital Ionograms Using Convolutional Neural Networks

De La Jara C.
Instituto Geofísico del Perú
cdelajara@igp.gob.pe

Olivares C.
Pontificia Universidad Católica del Perú
cesar.olivares@pucp.pe

Abstract—An ionogram is a graph that shows the distance that a vertically transmitted wave, of a given frequency, travels before returning to the earth. The ionogram is shaped by making a trace of this distance, which is called virtual height, against the frequency of the transmitted wave. Along with the echoes of the ionosphere, ionograms usually contain a large amount of noise and interference of different nature that must be removed in order to extract useful information. In the present work, we propose to use a convolutional neural network model to extract ionospheric layers profiles, improving the quality of the information obtained from digital ionograms, compared to that using image processing and machine learning techniques in the generation of electronic density profiles.

I. INTRODUCTION

Ionosondes are a type of radar that send pulses of high frequency radio waves to the ionosphere in the vertical direction. The echoes of these pulses are recorded on the ground and are used to generate a type of representative traces of the ionosphere, called ionograms. There is a direct relation between the frequency of the transmitted pulses and the ionization densities of the ionospheric layers that reflect them[1].

Echoes form characteristic patterns, which comprise an ionogram. The speed of the pulses traveling in the ionosphere is lower than the speed of the pulses traveling in free space, therefore, after a complete trip, it is possible to obtain information about the apparent height or virtual height of the layers. Critical frequencies are the limiting frequencies at which a wave is reflected by an ionospheric layer. Waves of frequencies above them penetrate through the layers. From ionograms it is possible to scale, manually or by computational methods, characteristic values of virtual heights $h'E$, $h'F$, $h'F_2$, etc and critical frequencies f_oE , f_oF_1 , f_oF_2 , etc of each layer of the ionosphere[2].

Interest in scaling and interpreting ionograms is increasing among the scientific community, the difficulty of these processes is that extracting ionospheric parameters through manual scaling is a very demanding task in both effort and time. With the development of image processing techniques, advances have been made in automatically scaling ionograms[3] [4], in which emphasis is mainly on the recognition of the ionogram traces, then obtaining density profiles applying ionospheric inversion techniques. In situations of high complexity, as in the case of incomplete ionograms or with the presence

of ionospheric phenomena such as spread F, automatic scaling becomes more difficult and tends to fail[5].

In the present work we propose the use of a convolutional neuronal network model for the detection of ionosphere echoes in digital ionograms, which can serve as a tool for automatic scaling.

The work is structured as follows: Section 2 gives a brief introduction to the operation mode of ionosondes, as well as characteristics of the ionosphere. Section 3 describes the characteristics of the data set used, how it was obtained and what pre processing was done. Section 4 describes the performance metric to be used. Section 5 describes and evaluates the performance of the baseline models. Section 6 describes the use of convolutional neural networks for profile detection.

II. THE IONOSPHERE

Ionograms show the time it takes for a wave of a certain frequency to be reflected by the ionosphere. An ionogram is a representation of the state of the ionosphere at a given time.

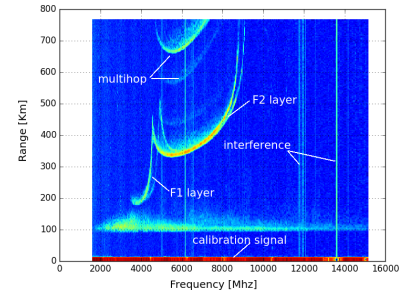


Fig. 1. Ionogram of Jicamarca ionosonde showing the virtual ionospheric height (vertical) versus frequency of transmitted pulses (horizontal). The traces show F1 and F2 layers as well as multihop, interference and calibration signal.

Figure 1 shows an example of a typical ionogram. Horizontal axis represents the frequencies of the transmitted radio signals and the vertical axis the virtual heights of ionospheric layers. The color of the trace is proportional to the intensity of the received signal, more intense echoes will have colors closer to red, while weaker echoes to blue. In this image it can also be clearly distinguished F1 layers over a height of 200 km and F2 over 300 km.

The ionosphere is a part of the earth's upper atmosphere, extending in height from 60 to about 1000 km. This region is composed of ionized gas, called plasma. The upper limit of the

ionosphere is defined as the height at which the concentration of charged particles of plasma, ions and electrons, exceed the concentration of neutral atoms and molecules, at this point the ionosphere begins to continuously transform into the magnetosphere, which it is a medium consisting only of strongly ionized plasma and intense electric and magnetic fields.

The ionosphere is formed when incident solar radiation removes electrons from gases of the upper atmosphere, creating electrically charged ions and free electrons. The ionization becomes greater when high energy radiation interacts with a greater density of air, and decreases when radiation loses intensity as it travels down the atmosphere.

Usually the ionosphere is divided into five independent regions, called layers. The lower layer, which ranges from 70 to 90 km in height, is called layer D; from 95 to 140 km is layer E, and above 140 km layer F. The latter is usually divided into two regions, F1, ranging from 140 to 200 km, and layer F2, which is above 200 km[6].

III. DATA SET DESCRIPTION

The data used for the training of the convolutional networks and the evaluation of the baseline models were obtained from the database of the distributed observatory LISN [7], which is a multi institution, multi instrument project in which a set of geophysical observation instruments have been deployed in different locations in South America in order to study the electrodynamics of the ionosphere, with emphasis on the dynamic energy transport and photo chemical processes, and also to develop the ability of predicting spread F occurrence and measurement of plasma densities, drifts and neutral winds in a large geographic area [8].



Fig. 2. The dots represent the geographic distribution of the ionosondes of the LISN distributed observatory, nearly aligned with the magnetic flux tube intersecting the magnetic equator at 70 deg West

Among the instruments used in the project there are 4 VIPIR ionosondes, in the cities of Lima and Puerto Maldonado in Peru, Tupiza in Bolivia and Tucuman in Argentina, whose ionograms will make up the data set. The data generated by these instruments have two objectives: education and scientific

research, they are freely available [9] and can be downloaded from the project website.

The data output of the VIPIR ionosondes is a Raw In-phase and Quadrature (RIQ) file that contains a number of range gate samples of the output of the Digital Down Converter for each of the 8 radar receive channels. These define the instrument mode of operation and the site specific information such as station location and antenna configuration. RIQ files are binary files with a specific, custom format [10]. RIQ FILES are converted and stored in NetCDF (ngi) format [11]. Ngi files store the required information to decode and plot ionograms, such as radar configuration, pulse configuration table and IQ data blocks.

The LISN database contains more than 900,000 ionograms. Depending on the geographical location and the type of experiment performed, the configuration of the ionosondes may vary, so the number of frequency and height points is not constant throughout the database. A group of 50,780 ionograms from the Jicamarca station was chosen to train the model, this ionograms were taken between 15:00 and 22:00 hours GMT from years 2016 to 2018. All of the ionograms chosen have 512 height and 408 frequency points. From this set, 817 were randomly selected to manually extract ionosphere profiles, we call this manual extraction, these files made up the labeled data set.

Figure 3 shows an ionogram before and after being manually converted to a binary image, in which the ionosphere profile has been extracted.

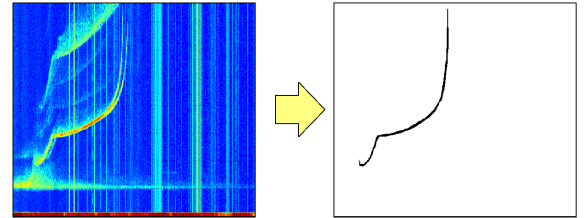


Fig. 3. Ionogram before and after been manually converted to a binary image

IV. PERFORMANCE METRICS

In this work we propose a method to extract ionospheric layers from digital ionograms using image segmentation with convolutional neural networks, where the main goal is to label every pixel of the image as belonging to the ionosphere trace or belonging to the background.

The most common performance metrics used for object segmentation problems is an index called intersection over union (IoU)[12]. IoU gives a ratio between the number of pixels common in two images and the total number of pixels in both images. If the images are exactly the same the result of this ratio would be 1, if there were few coincidences between the images (very different images) the result would be close to 0.

$$IoU = \frac{common_area}{total_area} \quad (1)$$

Since we are working with binary matrices the area is obtained by making a sum of all the cells in the matrix. The intersection will be obtained by performing a logical AND operation between the bits of the matrices and the union will be obtained by performing a logical OR.

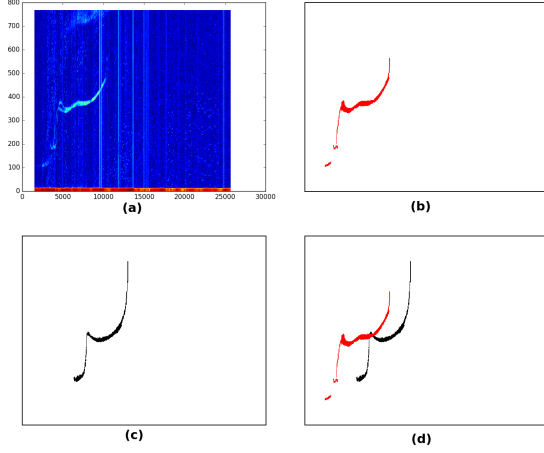


Fig. 4. (a) Original ionogram, (b) Manual segmentation, (c) Automatic segmentation, (d) Comparison between manual and automatic segmentation

Figure 4 shows the comparison of a manual segmentation (red) with automatic segmentation (black). In this case, at the bit level, the intersection matrix will have only a few cells in 1, resulting in an IoU close to zero. Manually segmented ionograms are considered to be perfectly segmented.

V. IMPLEMENTATION AND EVALUATION OF BASELINE MODELS

A. Profile detection using image processing and thresholding

In this approach, ionograms are considered as images, in which noise and interference must be filtered out to isolate ionospheric echoes. For this purpose, original ionograms are passed through three filters:

- Median filter
- Thresholding.
- The filter defined by the matrix K.

$$K = \begin{bmatrix} 1 & 1 & 1 & 0 & 1 & 1 & 1 \\ 1 & 1 & 1 & 0 & 1 & 1 & 1 \\ 1 & 1 & 1 & 0 & 1 & 1 & 1 \\ 1 & 1 & 1 & 0 & 1 & 1 & 1 \\ 1 & 1 & 1 & 0 & 1 & 1 & 1 \\ 1 & 1 & 1 & 0 & 1 & 1 & 1 \end{bmatrix} \quad (2)$$

As shown in figure 5, after passing through the three filters it is possible to accurately eliminate the background noise from ionograms, but neither the interference, nor the calibration signal nor multihop can be eliminated.

Average IoU between ionograms where the three filters were applied and manually segmented ionograms is 0.163.

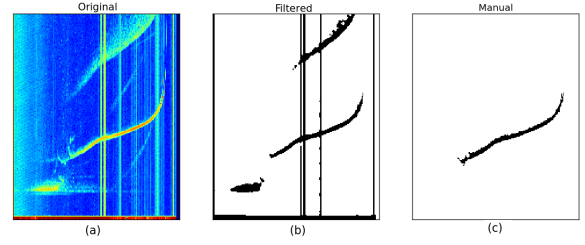


Fig. 5. Comparison between the original ionogram (a), the result of the cascade application of the K filter, median filter and thresholding (b) and a manually segmented ionogram (c)

B. Profile detection using unsupervised machine learning models

The other method is based on the representation of the ionograms in 3-dimensional matrices $\{x, y, V\}$ where x and y represent spatial coordinates and V the intensity of the point. With this representation two unsupervised clustering techniques are applied, K-Means and Mean Shift.

Clustering is a grouping technique to find, within a set of samples, groups that have similar characteristics, so samples that share comparable features will belong to the same group, and will be separated from other groups. The goal is to maximize variations between groups and minimize variations inside groups[13].

1) *K-means clustering*: K-means is a non supervised learning clustering technique that searches patterns in the data without having a specific prediction as a goal. K-means needs as input the number of groups (k) in which the samples will be segmented. Knowing this the algorithm places k random points as center of clusters, then assigns to this points the samples with the shortest distances, then the point shifts in the direction of the closest average distance, this process is repeated iteratively and the groups are adjusted until the centroid does not change further by moving the points. One of the K-means algorithm drawbacks is that it requires the number of clusters to be specified before the algorithm is applied. In this work we consider that a number of clusters equal to two reflects a specific characteristic of the data set, since we want to cluster the ionogram points into two main classes, ionospheric echoes and background noise. Figure 6 shows a comparison between an original ionogram, an ionogram segmented using K-means and a manually segmented ionogram. As with the application of the filters, interference, multihop and calibration signals are not removed.

Average IoU between ionograms segmented using K-means and manually segmented ionograms for the test set is 0.157.

2) *Mean shift clustering*: Mean shift is also a non supervised learning clustering technique that assigns the samples to the clusters by moving the center of these towards the direction of highest density of samples [14]. Giving a data set, mean shift is the displacement of a point from an initial location in the space, to another that results from the average of the weights of the data within a neighborhood determined by a region centered in x . Unlike K-Means algorithm, mean

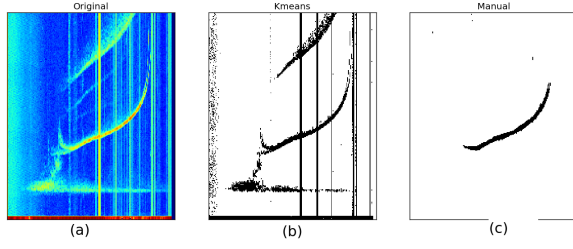


Fig. 6. Comparison between the original ionogram (a), application of K-means (b) and a manually segmented ionogram (c)

TABLE I
BASELINE MODELS AVERAGE IOU

	Filtered	K-Means	Mean Shift
IoU	0.163	0.157	0.105

shift does not require a previous knowledge of the number of clusters, they are determined by the algorithm with respect to the data.

Figure 7 shows a comparison between an original ionogram, a segmented ionogram using mean shift and a manually segmented ionogram.

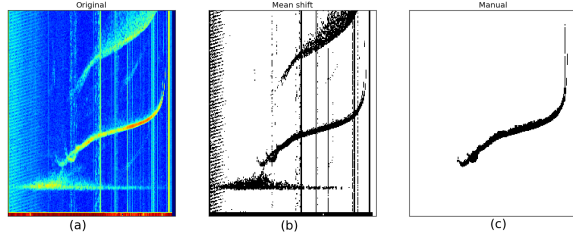


Fig. 7. Comparison between the original ionogram (a), application of mean shift (b) and a manually segmented ionogram (c)

Average IoU between ionograms segmented using mean shift and manually segmented ionograms for the test set is 0.105

Table I summarizes the results of the IoU for the three baseline models.

VI. PROFILES DETECTION USING CONVOLUTIONAL NEURAL NETWORKS

A large amount of unlabeled data is available from the LISN data base, on the other hand, labeled data can only be obtained by performing manual segmentation of ionograms, which is not only a time consuming process but also requires a high level of knowledge and experience. Given this scenario, with the goal of building a semi-supervised learning model, both types of data have been used, the large amount of unlabeled data and the small number of labeled (manually segmented) ionograms.

We used a model based on a multilayer convolutional encoder decoder neural network, with multiple layers of convolutions. The first part of the network is an encoder that

maps raw inputs to a rich representation of feature vectors, the second part is a decoder that takes these feature representation as input, process it, produces an output and maps the output back into the raw format. The network goal is to learn an efficient representation of the data.

Layer (type)	Output Shape	Param #
input_3 (InputLayer)	(None, 256, 208, 1)	0
conv2d_15 (Conv2D)	(None, 256, 208, 16)	160
max_pooling2d_7 (MaxPooling2)	(None, 128, 104, 16)	0
conv2d_16 (Conv2D)	(None, 128, 104, 8)	1160
max_pooling2d_8 (MaxPooling2)	(None, 64, 52, 8)	0
conv2d_17 (Conv2D)	(None, 64, 52, 8)	584
max_pooling2d_9 (MaxPooling2)	(None, 32, 26, 8)	0
conv2d_18 (Conv2D)	(None, 32, 26, 8)	584
up_sampling2d_7 (UpSampling2)	(None, 64, 52, 8)	0
conv2d_19 (Conv2D)	(None, 64, 52, 8)	584
up_sampling2d_8 (UpSampling2)	(None, 128, 104, 8)	0
conv2d_20 (Conv2D)	(None, 128, 104, 16)	1168
up_sampling2d_9 (UpSampling2)	(None, 256, 208, 16)	0
conv2d_21 (Conv2D)	(None, 256, 208, 1)	145
Total params: 4,385		
Trainable params: 4,385		
Non-trainable params: 0		

Fig. 8. Neural network model

Figure 8 shows a description of the network model. We use six convolutional layers with ReLU activation, three max poolings with zero padding and three up samplings. Binary cross entropy is used as loss function and adadelta as optimizer.

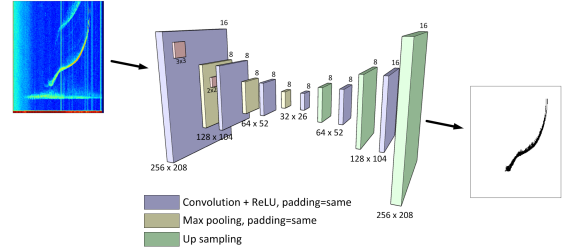


Fig. 9. Layers of the neural network model

Figure 9 shows details of the different layers of the neural network model.

The training set used has 31,699 ionograms, the validation set 9,577 and the test set 9,505. 816 ionograms were manually scaled, from them 474 are used as training set, 151 as validation set and 191 as test set.

A. Pre training: Building a neural network model from base line models

In the first stage of the learning process we feed the neural network with original ionograms (X) from the training/validation sets, and use as output variables (y) ionograms

TABLE II
CONVOLUTIONAL NETWORK AVERAGE IOU

	Filtered	K-Means	Mean Shift
IoU	0.174	0.173	0.077

that have been segmented using the three baseline techniques (filters, k-means and mean shift). We end up with three neural network models, each one learned to reconstruct ionograms the same way baseline models do it, as shown in figure 10.

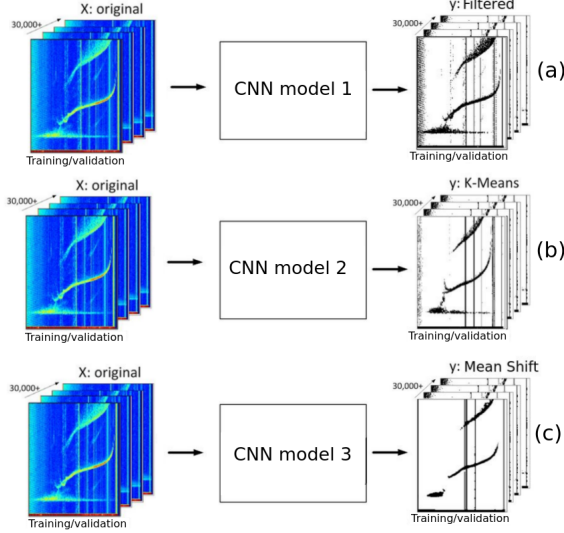


Fig. 10. Input data of all models are original ionograms. (a) CNN model 1: output variables are ionograms segmented using filters. (b) CNN model 2: output variables are ionograms segmented using K-means. (c) CNN model 3: output variables are ionograms segmented using mean shift.

The application of each of these models in the test set compared to manually segmented ionograms is shown in figure 11

Average IoU between ionograms segmented with these CNN models and manually segmented ionograms is summarized in table II. A small improvement is observed compared to IoU of baseline models.

B. Fine tuning: using manually segmented ionograms to improve performance of CNN models

In the second stage of the learning process, we fine tune the previously trained models. The three models are fed again with original ionograms from the training/validation sets, but the output variables this time are manually segmented ionograms from the training/validation sets, as shown in figure 12.

Figure 13 shows results of the different stages of the training process. Columns from left to right: Original ionogram, ionogram segmented using a CNN trained with baseline models, manually scaled ionogram, ionogram segmented using the CNN models plus fine tuning. In the latter it is observed that interference, background noise, calibration signal from the radar and E layer have been completely removed.

Manually segmented ionogram
NN segmented ionogram

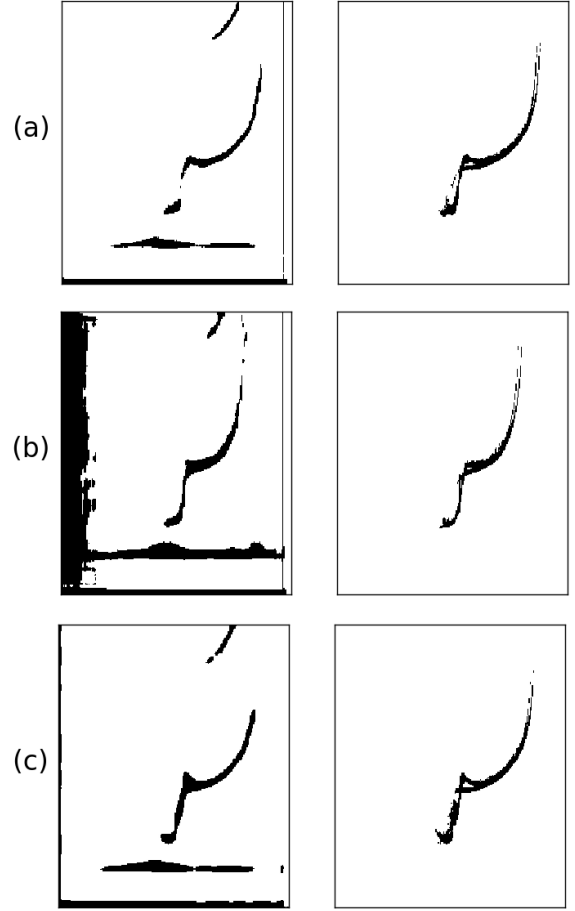


Fig. 11. Baseline model learning. Left column is the reconstruction of an ionogram using a neural network model trained with a base line model, and the right column is the manual segmentation of the ionogram. (a)Kmeans, (b)Mean shift (c)filters

TABLE III
FINE TUNED CONVOLUTIONAL NETWORK AVERAGE IOU

	Filtered	K-Means	Mean Shift
IoU	0.589	0.602	0.593

Average IoU between test set ionograms segmented with fine tuned models and manually segmented ionograms is summarized in table III. A significant improvement is observed compared with the IoU of ionograms segmented before applying fine tuning.

C. Building a neural network model from labeled ionograms only

As a final stage, another CNN model was created using only manually segmented ionograms as training data, no pre training was used. This model gives an average IoU of 0.569, which is unexpectedly high given the small amount of data used for training.

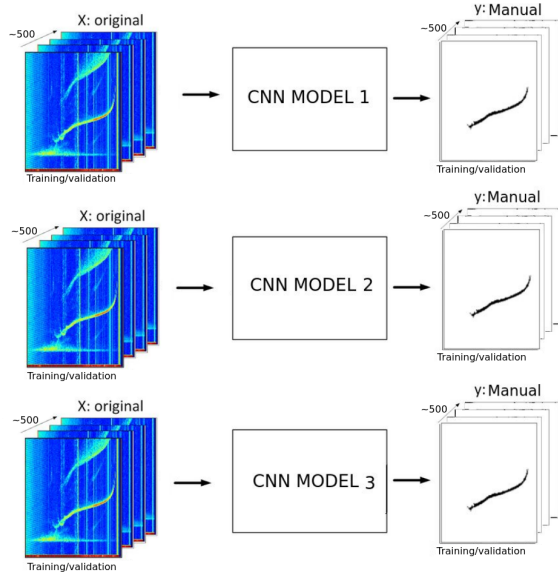


Fig. 12. Fine tuning of pre trained models. Input data of all models are original ionograms and output variables are manually segmented ionograms.

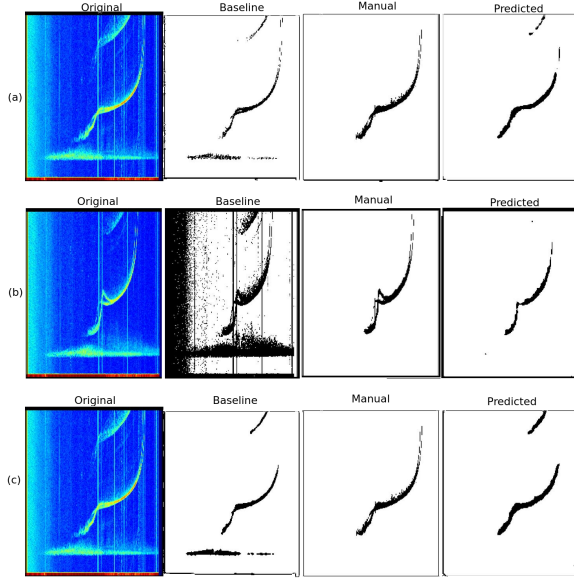


Fig. 13. Fine tuning and final prediction. (a)Kmeans, (b)Mean shift (c)filters

Average IoU of all models are summarized in figure 14.

Figure 15 shows examples of accurate predictions of unseen data (ionograms that do not belong to any of the sets used in the learning phase of the model development), showing good generalization performance.

Figure 16 shows inaccurate predictions on unseen data. This happens with ionograms that have weak traces, also with ionograms whose shapes have not been seen frequently during the training process. More manually scaled ionograms on a more diverse set of shapes should be created to reduce the number of inaccurate predictions.

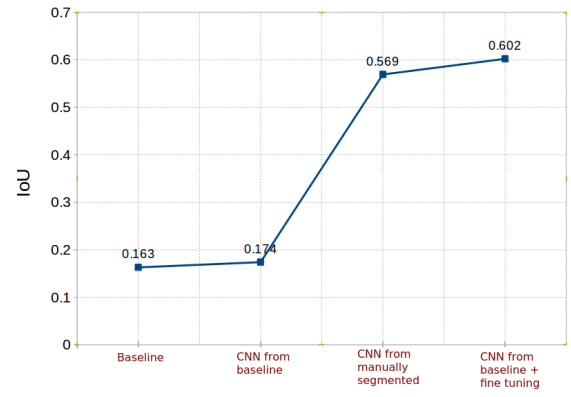


Fig. 14. Average IoU of all models

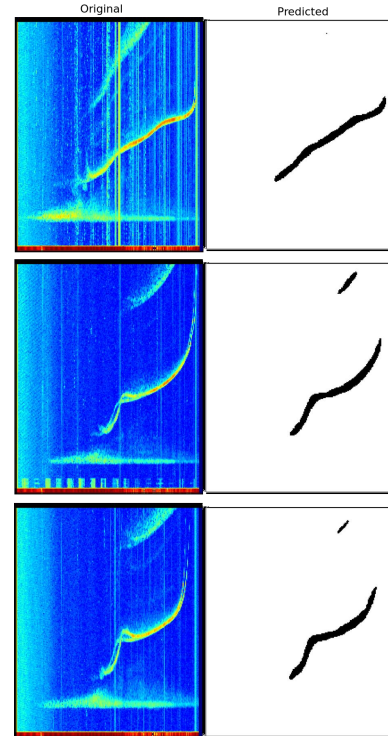


Fig. 15. Accurate predictions of unseen data

VII. CONCLUSIONS

- 1) In terms of IoU, segmentation of ionograms when using a neural network trained using labeled data is 5.6 times better than segmentation performed by baseline models.
- 2) The use of large amounts of unlabeled data to generate a pre-trained model slightly improves (<6%) the accuracy of the final model, so we can say that performance of the model is based mainly on the use of labeled data for training and not on a pre-training process with unlabeled data.
- 3) In order to improve model generalization, it is necessary to train it with a greater amount of labeled data, from a more diverse set of ionograms, from different periods

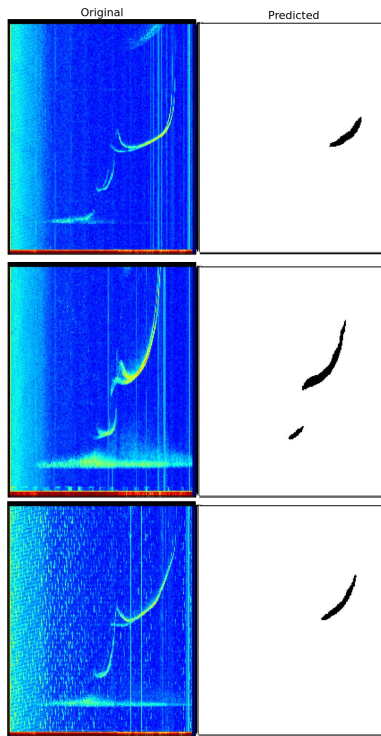


Fig. 16. Inaccurate predictions of unseen data

of time and geographic locations, covering a greater number of possible states of the ionosphere.

ACKNOWLEDGEMENT

The Low Latitude Ionospheric Sensor Network (LISN) is a project led by the University of Texas at Dallas in collaboration with the Geophysical Institute of Peru and other institutions that provide information in benefit of the space weather scientific community. We thank all organizations and persons that are supporting and operating receivers under the LISN project. All ionograms that were used to train the neural network models are available and can be downloaded from the following location <https://lisn.igp.gob.pe>.

REFERENCES

- [1] W. Piggot and K. Rawer, *URSI Handbook of Ionogram Interpretation and Reduction*. World Data Center for Solar-Terrestrial Physics, 1972.
- [2] L. Perrone, A. Mikhailov, C. Cesaroni, L. Alfonsi, A. De Santis, P. Michael, and C. Scotto, "Long-term variations of the upper atmosphere parameters on rome ionosonde observations and their interpretation," *J. Space Weather Space Clim*, 2017.
- [3] C. Scotto and M. Pezzopane, "A software for automatic scaling of fof2 and muf (3000) f2 from ionograms," *URSI XXVIIIth General Assembly*, 2002.
- [4] C. Ziwei, W. Shun, Z. Shunrong, F. Guangyou, and W. Jinsong, "Automatic scaling of f layer from ionograms," in *Radio Science*, vol. 48, 2013, pp. 334–343.
- [5] S. M. Stankov, J.-C. Jodogne, I. Kutiev, K. Stegen, and R. Warnant, "Evaluation of automatic ionogram scaling for use in real-time ionospheric density profile specification: Dourbes dgs-256/artist-4 performance," *Annals of Geophysics*, 2012.
- [6] A. S. Jursa, *Handbook of Geophysics and the Space Environment*. Air Force Geophysics Lab Hanscom AFB MA, 1985.

- [7] "observatorio distribuido lisn". Instituto Geofisico del Peru, 2019. Accessed: 2019-02-15. [Online]. Available: <http://lisn.igp.gob.pe>
- [8] C. E. Valladares and J. L. Chau, "The low-latitude ionosphere sensor network: Initial results," *Radio Science*, vol. 47, no. 4, May 2012. [Online]. Available: <https://doi.org/10.1029/2011rs004978>
- [9] "lisn data user rules". Instituto Geofisico del Peru, 2019. Accessed: 2019-02-15. [Online]. Available: <http://lisn.igp.gob.pe/data/>
- [10] T. Bullet. (2015) Software for reading VIPIR raw data files. National Oceanics and Atmospheric Administration. Accessed: 2019-01-15. [Online]. Available: <ftp://ftp.ngdc.noaa.gov/>
- [11] "network common data form (netcdf)". University Corporation for Atmospheric Research. Accessed: 2019-01-15. [Online]. Available: <https://www.unidata.ucar.edu/software/netcdf/>
- [12] M. A. Rahman and Y. Wang, "Optimizing intersection-over-union in deep neural networks for image segmentation," in *International Symposium on Visual Computing*. Springer, 2016, pp. 234–244.
- [13] D. Pham, S. Dimov, and C. Nguyen, "Selection of k in k-means clustering," *Journal of Mechanical Engineering Science 1989-1996 (vols 203-210)*, 2005.
- [14] Y. Cheng, "Mean shift, mode seeking, and clustering," *IEEE Transactions On Pattern Analysis And Machine Intelligence*, vol 17 no 8, 1995.